

Optical investigations on $Y_{2-x}Bi_xRu_2O_7$: Electronic structure evolutions related to the metal-insulator transition

J. S. Lee, S. J. Moon, and T. W. Noh

School of Physics and Research Center for Oxide Electronics, Seoul National University, Seoul 151-747, Korea

T. Takeda

Division of Materials Science and Engineering, Graduate School of Engineering, Hokkaido University, Hokkaido 060-8628, Japan

R. Kanno

Department of Electronic Chemistry, Interdisciplinary Graduate School of Science and Engineering, Tokyo Institute of Technology, Yokohama 226-8502, Japan

S. Yoshii* and M. Sato

Department of Physics, Division of Material Science, Nagoya University, Furo-cho, Chikusa-ku, Nagoya 464-8602, Japan

(Received 16 March 2005; published 18 July 2005)

Optical conductivity spectra of cubic pyrochlore $Y_{2-x}Bi_xRu_2O_7$ ($0.0 \leq x \leq 2.0$) compounds are investigated. As a metal-insulator transition (MIT) occurs around $x=0.8$, large spectral changes are observed. With increase of x , the correlation-induced peak between the lower and the upper Hubbard bands seems to be suppressed, and a strong mid-infrared feature is observed. In addition, the $p-d$ charge transfer peak shifts to the lower energies. The spectral changes cannot be explained by electronic structural evolutions in the simple bandwidth-controlled MIT picture, but are consistent with those in the filling-controlled MIT picture. In addition, they are also similar to the spectral changes of $Y_{2-x}Ca_xRu_2O_7$ compounds, which is a typical filling-controlled system. This work suggests that, near the MIT, the Ru bands could be doped with the easily polarizable Bi cations.

DOI: [10.1103/PhysRevB.72.035124](https://doi.org/10.1103/PhysRevB.72.035124)

PACS number(s): 71.30.+h, 78.20.-e, 78.40.-q

I. INTRODUCTION

Pyrochlore ruthenium oxides $A_2Ru_2O_{7-\delta}$ [$A=Bi, Tl, Pb, Y,$ and $L(=Pr-Lu)$] are interesting materials, which show numerous electronic properties depending on the A -site ions. While $Bi_2Ru_2O_7$ and $Pb_2Ru_2O_{6.5}$ are good metals, $Y_2Ru_2O_7$ and $L_2Ru_2O_{7-\delta}$ are insulators.¹⁻³ On the other hand, $Tl_2Ru_2O_7$ shows a temperature-dependent metal-insulator transition (MIT) around 125 K.⁴ Therefore, it is clear that the electronic structures, especially near the Fermi level (E_F), should have some systematic evolutions depending on the A -site ions. Numerous investigations have been made to understand how the electronic structures will evolve in these pyrochlore ruthenates,⁵⁻¹⁴ however, there is no real consensus on this issue yet.

One explanation is based on the fact that the different sizes of the A -site ions will control structural properties, such as Ru—O—Ru bond angle, which result in bandwidth changes of the Ru t_{2g} bands. With strong electron-electron correlation effects,^{5-7,10-12} these changes could result in a MIT, called the “bandwidth-controlled MIT.” In the early days, Cox *et al.* investigated $Bi_2Ru_2O_7$, $Y_2Ru_2O_7$, and $Pb_2Ru_2O_{6.5}$ by using photoemission spectroscopy and high-resolution electron-energy-loss spectroscopy and found that the density of states at E_F should decrease in the sequence of $Pb_2Ru_2O_{6.5}$, $Bi_2Ru_2O_7$, and $Y_2Ru_2O_7$.⁵ They concluded that $Y_2Ru_2O_7$ should be in the insulating state due to correlation-induced electron localization, namely the Mott insulator. Lee *et al.* calculated the bandwidth of the Ru t_{2g} bands using an extended Huckel tight binding method and confirmed that

the MIT in the pyrochlore ruthenates should originate from the change of the relative size between the correlation energy and bandwidth, which was controlled by the A -site ion size.⁷

The other explanation is based on the fact that Pb or Bi $6p$ electrons should have very large wave functions, which could hybridize with the Ru t_{2g} wave functions. This hybridization could result in large bandwidths of the Ru t_{2g} bands and a net transfer of charge to the Ru t_{2g} bands,⁸⁻¹¹ so the ruthenates could experience a MIT, called the “filling-controlled MIT.” Hsu *et al.* compared the x-ray photoemission spectroscopy spectra of $Pb_2Ru_2O_{6.5}$ and $Bi_2Ru_2O_7$ with band-structure calculations and argued that the unoccupied Pb or Bi $6p$ states should be closely related to their metallic conductivity through mixing with the Ru $4d$ states via the ligand oxygen $2p$ states.⁸ Later, using the LDA calculation on $A_2Ru_2O_{7-\delta}$ ($A=Bi, Tl,$ and Y), Ishii and Oguchi also obtained similar results that the Bi $6p$ and the Tl $6s$ states could hybridize with the Ru t_{2g} states and should contribute to the density of states at E_F .⁹ Considering the fact that the formal charge valences of Pb and Bi are +3 just like those of the other pyrochlore ruthenates, the filling-controlled MIT is rather surprising. Consequently, it is important to discriminate whether the metallic state of the pyrochlore ruthenates originates from the large bandwidth of the Ru $4d$ bands or from the filling change.

Optical spectroscopy has been used as a powerful tool to investigate electronic structures of highly correlated electron systems.^{15,16} Several optical studies have been already done on some pyrochlore ruthenates and provided some clues to understanding of their electronic structure changes.^{10,17-19}

Earlier, we compared the optical spectra of $Y_2Ru_2O_7$, $CaRuO_3$, $SrRuO_3$, and $Bi_2Ru_2O_7$, and we already showed that $Y_2Ru_2O_7$ should be a Mott insulator and that the metallic states of the perovskites could be understood in the bandwidth control picture.¹⁰ However, we stated that the metallic state of the pyrochlore $Bi_2Ru_2O_7$ could not be easily understood. (See comment 32 in Ref. 10.)

In this paper, we report the optical conductivity spectra $\sigma(\omega)$ of $Y_{2-x}Bi_xRu_2O_7$ (YBRO) ($x=0.0, 0.5, 1.0, 1.5,$ and 2.0). YBRO is a good model system to investigate the MIT mechanism of the pyrochlore ruthenates, since it has both insulating and metallic end members. In addition, its solid solution can be easily formed in all the region of x , and a MIT occurs around $x=0.8$.^{2,3} When the YBRO compound becomes metallic, the structural symmetry remains as a cubic; however, with increase of x , the Ru—O bond length decreases and the Ru—O—Ru bond angle increases.² These x dependences are consistent with those in other pyrochlore ruthenates.^{13,14,20,21} From the room temperature $\sigma(\omega)$ of YBRO, we observed that the variation of x could result in systematic spectral changes, including large peak shifts and spectral weight redistributions in a wide energy range up to 5 eV. Using these spectral changes, we will address the MIT of YBRO from the bandwidth- and filling-controlled pictures. To clarify our argument further, we will also compare $\sigma(\omega)$ of YBRO with those of $Y_{2-x}Ca_xRu_2O_7$, which is a typical filling-controlled system.²²

II. EXPERIMENTAL

Polycrystalline $Y_{2-x}Bi_xRu_2O_7$ samples were synthesized using the solid state reaction method.² Since the pyrochlore phase has a cubic structure, optical constants of the pyrochlore ruthenates should be isotropic, so we can determine their optical constants from the reflectivity measurements of polycrystalline samples. Before reflectivity measurements, the sample surfaces were polished up to $0.3 \mu\text{m}$. We measured reflectivity spectra from 5 meV to 30 eV using numerous spectrophotometers.¹⁰ After the optical measurements, thin gold films were evaporated on the samples and their reflectivity spectra were measured again to correct the errors due to scattering from the sample surfaces.²³ From the reflectivity spectra, we performed the Kramers-Kronig (K-K) analysis to obtain $\sigma(\omega)$. For this analysis, the reflectivity below 5 meV was extrapolated with a constant value for the insulating samples and the Hagen-Rubens relation for the metallic samples. Note that the dc conductivity values used for the Hagen-Rubens relation are larger by about two times the values obtained by the four-probe method, which originates from the polycrystalline effects in the latter measurement.²⁴ For a high-frequency region, the reflectivity value at 30 eV was used for reflectivities up to 40 eV, above which ω^{-4} dependence was assumed. In addition, we also independently measured $\sigma(\omega)$ between 0.7 and 4.0 eV using spectroscopic ellipsometry. The results of the K-K analysis agreed with the ellipsometry data, demonstrating the validity of our K-K analysis.²³

Sintered polycrystalline samples of $Y_{2-x}Ca_xRu_2O_7$ were also synthesized by the solid reaction.²² The sample densities

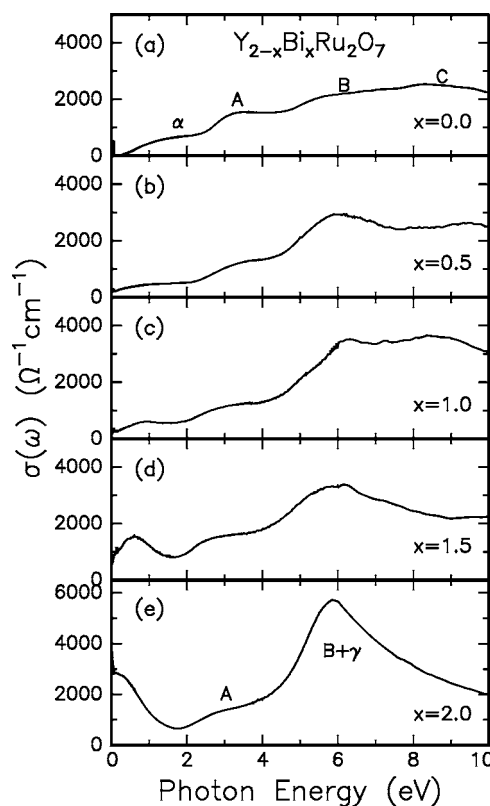


FIG. 1. Doping-dependent $\sigma(\omega)$ of $Y_{2-x}Bi_xRu_2O_7$ at room temperature up to 10 eV. The indices of each peak appearing in (a) and (e) indicate the corresponding optical excitations, displayed in Fig. 2.

were too low for the reflectivity measurements, so we decided to obtain their absorption spectra by measuring transmittance spectra of $Y_{2-x}Ca_xRu_2O_7$ particles embedded in a KBr matrix, which is transparent up to around 4 eV. Mixtures of $Y_{2-x}Ca_xRu_2O_7$ and KBr powders were mixed together thoroughly and pressed into pellets, whose thicknesses were about 1 mm. The transmittance spectra were measured between 0.5 and 4.0 eV, and the absorption spectra were evaluated by taking logarithms of the transmittance spectra and dividing them by the pellet thicknesses.²⁵

III. ASSIGNMENT OF SPECTRAL FEATURES OF $Y_{2-x}Bi_xRu_2O_7$ BASED ON THE ELECTRONIC STRUCTURES OF END MEMBERS

Figure 1 shows room temperature $\sigma(\omega)$ of $Y_{2-x}Bi_xRu_2O_7$ ($x=0.0, 0.5, 1.0, 1.5,$ and 2.0) up to 10 eV. For $x=0.0$, $\sigma(\omega)$ shows an insulating behavior with a small optical gap around 0.14 eV and the lowest interband transition around 1.6 eV.²⁶ It also shows strong peaks around 3, 6, and 9 eV. As x increases, two intriguing spectral changes can be observed. (1) The spectral weight below around 1.0 eV increases, and a strong Drude-like peak appears for $x=2.0$. These behaviors are consistent with the x dependence of dc resistivity.^{2,3} (2) While the strength of the 6 eV peak increases, that of the 9 eV peak decreases and almost disappears for $x=1.5$ and 2.0.

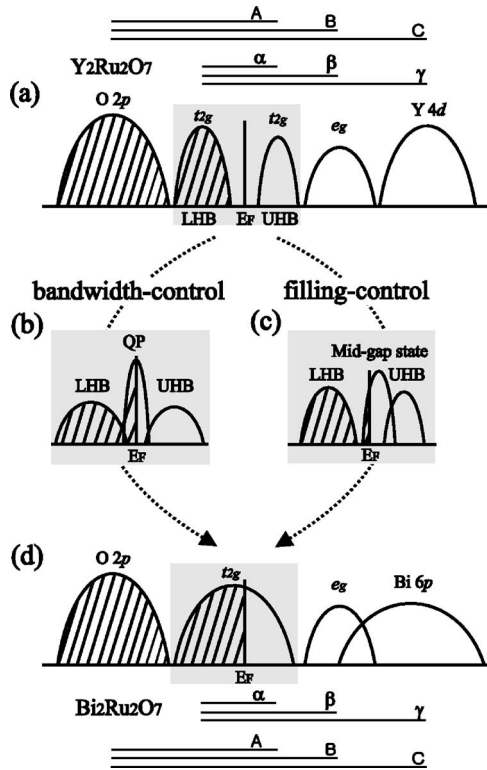


FIG. 2. Schematic diagrams of the electronic structures of $Y_{2-x}Bi_xRu_2O_7$ (a) corresponds to that for $x=0$, i.e., $Y_2Ru_2O_7$. The occupied and unoccupied Ru t_{2g} states are located near E_F , forming the lower Hubbard band (LHB) and the upper Hubbard band (UHB), respectively. Outside these Ru t_{2g} states, there are the occupied O $2p$ states and the unoccupied Ru e_g states and the Y $4d$ states. (b) sketches possible electronic structures of the Ru t_{2g} states in the intermediate region of $x \sim 1.0$, when a metal-insulator transition occurs through a change of the bandwidth. In the bandwidth-controlled system, a quasi-particle (QP) should appear between the Hubbard bands. (c) sketches electronic structures, when a metal-insulator transition occurs due to the doping. In the filling-controlled system, a mid-gap state should appear. (d) corresponds to electronic structures for $x=2.0$, i.e., $Bi_2Ru_2O_7$. Compared to (a), the Bi $6p$ state replaces the Y $4d$ state, and the t_{2g} states form a single peak centered near E_F . In (a) and (d), possible optical transitions are also indicated as A, B, C, α , β , and γ .

In order to understand spectral weight changes more easily, let us adopt the schematic diagrams for the electronic structures of the end members, i.e., $Y_2Ru_2O_7$ and $Bi_2Ru_2O_7$, which were already presented in Ref. 10, and also displayed in Figs. 2(a) and 2(d), respectively. For $Y_2Ru_2O_7$, the Ru ion has its formal valence of $4+$ with four t_{2g} electrons. Since it is known as a Mott insulator,^{5,10} the partially filled t_{2g} states split into the lower Hubbard band (LHB) and the upper Hubbard band (UHB),²⁷ as shown in the shaded area of Fig. 2(a).²⁸

The unoccupied e_g states are located above the t_{2g} states by a crystal field splitting energy of about 3 eV.¹⁰ The occupied O $2p$ states and the unoccupied Y $4d$ states are located below the LHB and above the e_g states, respectively. On the other hand, $Bi_2Ru_2O_7$ is close to a band metallic state,⁵ where the t_{2g} states form a single partially filled band at E_F ,

as shown in the shaded area of Fig. 2(d). Instead of the unoccupied Y $4d$ states in $Y_2Ru_2O_7$, $Bi_2Ru_2O_7$ will have the unoccupied Bi $6p$ states, whose bandwidth might be much larger due to the extended nature of their corresponding wave functions. Other states, including the O $2p$ states and the Ru e_g states, should remain nearly the same.

In each diagram, possible charge transfer excitations from the O $2p$ states are indicated as transitions A, B, and C, and possible transitions from the Ru t_{2g} states are indicated as transitions α , β , and γ . For $Y_2Ru_2O_7$, the lowest excitation around 1.6 eV can be assigned to the $d-d$ transition between the Hubbard bands, i.e., transition α . And, the strong peaks around 3, 6, and 9 eV can be assigned to transitions A, B, and C, respectively. For $Bi_2Ru_2O_7$, the coherent peak below 1.5 eV should be attributed to the intraband transition of the partially filled t_{2g} band, and the 3 eV peak can be assigned as transition A. The position of the 6 eV peak should correspond to the energies of transition B and an additional dipole-allowed transition, i.e., transition γ between the Ru t_{2g} states and the Bi $6p$ states. The contributions from these two transitions can explain the large strength of this spectral feature.

The general trends of the high energy spectral changes, shown in Fig. 1, can be understood based on the electronic structures of $Y_2Ru_2O_7$ and $Bi_2Ru_2O_7$. Note that, as the Bi content increases, the 6 eV peak gains its spectral weight, and the 9 eV peak loses its spectral weight. These systematic x dependences confirm our peak assignments that the peaks around 6 and 9 eV should be related to the Bi ion states and the Y ion states, respectively. Based on these peak assignments, we can argue that the spectral features in the low energy region below 5 eV should come from optical transitions related to the Ru t_{2g} and the O $2p$ states.

IV. POSSIBLE MODELS FOR ELECTRONIC STRUCTURAL EVOLUTIONS OF $Y_{2-x}Bi_xRu_2O_7$: BANDWIDTH- VS. FILLING-CONTROL

Figures 2(b) and 2(c) show the possible electronic structures near E_F for the intermediate compounds between $Y_2Ru_2O_7$ and $Bi_2Ru_2O_7$ in the bandwidth- and the filling-controlled MIT pictures, respectively. The electronic structures in the high energy regions are not displayed, since they should exhibit normal x dependences; that is, as x increases, while the O $2p$ states and the Ru e_g states would not be much affected, the Y $4d$ states should be replaced by the Bi $6p$ states. On the other hand, the details of the Ru t_{2g} states near E_F should change according to the mechanisms of the MIT.

First, let us consider the bandwidth-controlled MIT, where the quasi-particle (QP) peak should appear near E_F between LHB and UHB,²⁷ as displayed in Fig. 2(b). When the system becomes more metallic, the QP peak should increase with the reductions of the Hubbard bands. The corresponding $\sigma(\omega)$ in the low energy region should be composed of three spectral features: (i) a coherent peak centered at zero energy, (ii) an incoherent excitation between the Hubbard bands, and (iii) strong $p-d$ transitions located at the higher energies. As shown in the inset of Fig. 3, $\sigma(\omega)$ of $CaRuO_3$,¹⁰ which is known to be a correlated metal, exhibits such spectral fea-

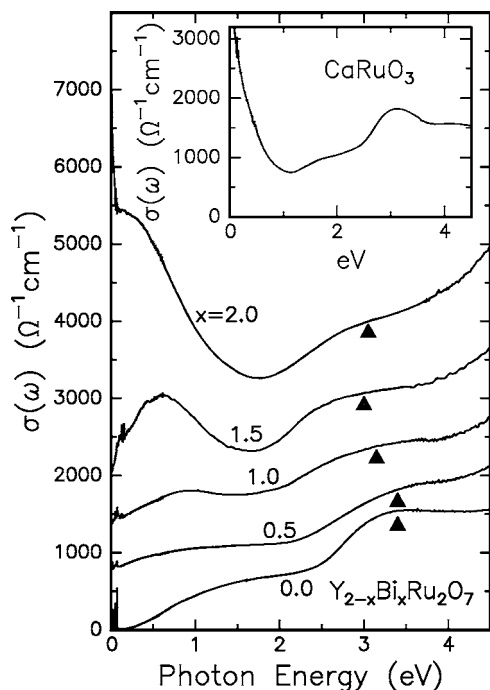


FIG. 3. Doping-dependent $\sigma(\omega)$ of $Y_{2-x}Bi_xRu_2O_7$ at room temperature up to 4.5 eV. The spectra for $x=0.5, 1.0, 1.5,$ and 2.0 are shown with an upward shift by 600, 1200, 1500, and 2600 $\Omega^{-1} \text{cm}^{-1}$, respectively. Inset shows $\sigma(\omega)$ of $CaRuO_3$ at room temperature.

tures quite well: namely, the Drude-like peak in the zero energy limit, the correlation-induced peak around 1.8 eV, and the $p-d$ transition peaks above 3 eV. As the system approaches the band metallic state, the coherent peak should develop, accompanied by the reduction of the incoherent excitation.

Second, let us look into the filling-controlled MIT, where a mid-gap state should appear just below UHB (above LHB) for the hole (electron) doping case,²⁷ as displayed in Fig. 2(c). Different from the QP peak in the bandwidth-controlled picture, this mid-gap state is not centered around E_F , and it should provide an incoherent transport behavior in a moderate doping regime due to the disorder-induced carrier localization.¹⁶ In the hole-doping case, $\sigma(\omega)$ should have two additional excitations to the mid-gap state from LHB and from the O $2p$ states, each of which should appear at lower energies than transitions α and A, respectively. As the carrier doping increases, the excitations to the mid-gap state should become stronger, accompanied by spectral weight reductions of transitions α and A. It should be noted that the lowest excitation comes from the transition between the LHB and the mid-gap state, so that it should have a peak center at a finite energy. Considering large differences in the electronic structures near E_F and the corresponding $\sigma(\omega)$ between the bandwidth- and filling-controlled MIT pictures, we will be able to address the possible MIT mechanism of YBRO by investigating their spectral changes at the low energy region.

V. DISCUSSIONS ON THE METAL-INSULATOR TRANSITION MECHANISM OF $Y_{2-x}Bi_xRu_2O_7$

A. Spectral changes of YBRO below 4.5 eV

In order to investigate how the electronic structures of YBRO evolve near E_F as the MIT occurs, we look into their $\sigma(\omega)$ in the low energy region. Figure 3 shows $\sigma(\omega)$ of YBRO up to 4.5 eV. As the MIT occurs, large spectral changes are observed for both the $d-d$ and the $p-d$ transitions. For the $d-d$ transitions, while $\sigma(\omega)$ of the $x=0.0$ compound exhibits the correlation-induced peak around 1.6 eV, $\sigma(\omega)$ of the $x=2.0$ compound does not show the correlation-induced peak but exhibits a strong Drude-like peak extending up to 1.5 eV. For the $x=1.0$ and 1.5 compounds, strong incoherent mid-infrared peaks can be observed. On the other hand, the $p-d$ transition shows a systematic redshift with increase of x , as indicated by the solid triangles. Considering the fact that the spectral features in this energy region should be mainly contributed by the Ru t_{2g} and the O $2p$ states, such systematic spectral changes with x indicate that there should be significant evolutions of these states near the MIT.

B. Discussions based on the bandwidth-control picture

Let us first discuss the evolution of $\sigma(\omega)$ of YBRO in the low energy region based on the bandwidth-control picture. Considering the x -dependent changes of the Ru—O bond length and the Ru—O—Ru bond angle,² we can expect that the Ru t_{2g} bandwidth should increase as x increases. Actually, the recent photoemission spectroscopy study on the Ru $3d$ core level by Kim *et al.* demonstrated that the electron correlation strength changes systematically with x , and it would play an important role in determining the electronic structures of YBRO.²⁹ In our optical data also, as discussed in Sec. III, the low energy spectral features of at least two end members, i.e., the $x=0.0$ and 2.0 compounds, seem to exhibit typical behaviors of the Mott insulator and the band metal, respectively.

However, when we look into the systematic changes of $\sigma(\omega)$ between end members, we can find a few intriguing features deviating from expected changes in the simple bandwidth-control picture. First, $\sigma(\omega)$ in the low energy region of the intermediate compounds with $x=1.0$ or 1.5 are much different from that of a so-called correlated metal. Assuming that the bandwidth-controlled MIT should occur in YBRO, the $x=1.0$ and 1.5 compounds could be considered as correlated metals located between the Mott insulator and the band metal. Then, according to the diagram in Fig. 2(b), their $\sigma(\omega)$ should exhibit a Drude-like peak centered at zero energy and a correlation-induced $d-d$ transition peak, which is observed for $x=0.0$ around 1.6 eV. Instead of such peak structures, they exhibit just a strong mid-infrared peak around 1.0 eV for $x=1.0$ (and 0.5 eV for $x=1.5$).

Second, the $p-d$ transition peak exhibits an unusual x -dependent evolution, which is different from typical behaviors of the bandwidth-controlled system. We estimated the energy position ω_{p-d} of the peak by fitting $\sigma(\omega)$ with a series of the Lorentz oscillators.¹⁰ As shown in Fig. 4(a), ω_{p-d} shows a gradual decrease with increase of x . Note that

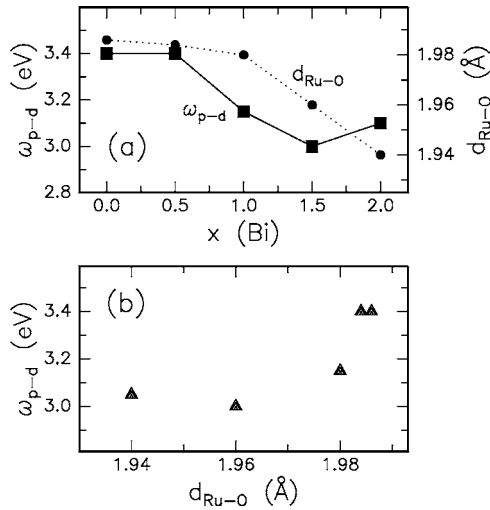


FIG. 4. (a) Doping-dependent changes of the $p-d$ transition energy ω_{p-d} and (b) Ru—O bond length d_{Ru-O} dependence of ω_{p-d} .

the Ru t_{2g} bandwidth should be largely influenced by the $p-d$ hybridization between the O $2p$ and Ru t_{2g} states. If the $p-d$ hybridization plays an important role, ω_{p-d} should be largely determined by the Ru—O bond length d_{Ru-O} : ω_{p-d} should be inversely proportional to d_{Ru-O} .^{30–32} Namely, the smaller d_{Ru-O} would make the larger energy splitting between the O $2p$ states and the Ru t_{2g} states, resulting in larger ω_{p-d} . On the contrary to this expectation, ω_{p-d} decreases with decrease of d_{Ru-O} ,² as shown in Fig. 4(b). This indicates that the observed d_{Ru-O} dependence of ω_{p-d} could not be simply related to the bandwidth-control effects.³³

C. Discussions based on the filling-control picture

In fact, the filling-controlled MIT picture can provide good explanations for most of the observed spectral changes of $\sigma(\omega)$ in the low energy region. As shown in Fig. 3, the $d-d$ transitions and the $p-d$ transitions for the intermediate compounds with $x=0.5$ and 1.0 seem to be broader than those of end members. And, as x increases, both of them look like shifting to the lower energies. According to the schematic diagram in Fig. 2(c), which supposes the hole doping case for the Ru ions, the mid-gap state becomes stronger with an increase of the hole doping for the Ru ions. Then the intermediate compounds should have two additional optical excitations, and each of them should be located just below transitions α and A of the $x=0.0$ compound. This explains why the $d-d$ and the $p-d$ transitions for the intermediate compounds become broader. If the finite widths of the peaks are taken into consideration, the apparent redshifts of the $d-d$ and $p-d$ transitions could be attributed to the increased spectral weights of such additional excitations.

Moreover, the d_{Ru-O} dependence of ω_{p-d} , shown in Fig. 4(b), is also consistent in the filling-controlled picture. As x increases, the amount of hole doping for the Ru ions increases, so d_{Ru-O} could decrease.^{13,14} In addition, with the increase of x , the mid-gap state becomes stronger, resulting in the apparent redshifts of ω_{p-d} , as we addressed in the

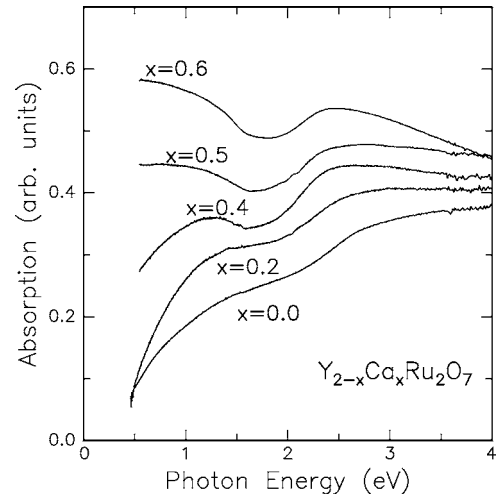


FIG. 5. Absorption spectra of $Y_{2-x}Ca_xRu_2O_7$ at room temperature. All of the spectra are shown in arbitrary units.

above paragraph. Therefore, ω_{p-d} will decrease at smaller d_{Ru-O} .

Although the filling-controlled MIT picture is consistent with the observed spectral changes of YBRO, it should be noted that the low frequency spectral distribution of YBRO is too broad to clearly identify the appearance of the mid-gap state. In recent photoemission studies, Park *et al.* observed an increase of the spectral weight near E_F ,¹² but the spectral features in the photoemission spectra were also too broad to clearly distinguish the appearance of the mid-gap state. The broad spectral features in the mid-infrared peak and the photoemission spectra might be related to the extended nature of the Bi $6p$ orbitals,^{8–10} which are hybridized with the Ru t_{2g} bands.

D. Comparison with the spectral changes of $Y_{2-x}Ca_xRu_2O_7$, a filling-controlled system

To obtain further supports for the possible scenario of the YBRO MIT mechanism, we investigated absorption spectra of $Y_{2-x}Ca_xRu_2O_7$ (YCRO), which shows a MIT around $x=0.5$.²² Since Y and Ca ions have different ionic states, as $3+$ and $2+$, respectively, the hole doping for the Ru $4d$ states should occur and increase with the increase of x . Therefore, the YCRO compounds will work as a model system with a clear filling-controlled MIT.

Figure 5 shows the absorption spectra of the YCRO compounds between 0.5 and 4 eV. The spectra below 0.5 eV could not be measured due to the multi-phonon absorption of the KBr pellet. For the $Y_2Ru_2O_7$ sample, its absorption spectrum is quite similar to its $\sigma(\omega)$, displayed in the bottom of Fig. 3, demonstrating the validity of our approaches using transmittance spectra. It is quite interesting to find that x -dependent changes of the absorption spectra for YCRO compounds are quite similar to those of $\sigma(\omega)$ for the YBRO compounds, shown in Fig. 3. Characteristic spectral features in YBRO, i.e., the redshifts of the $d-d$ transition peak and the $p-d$ transition peak, can also be observed in the absorption spectra of YCRO. These similarities of optical spectra

between YBRO and YCRO strongly support our proposal that the MIT of the YBRO should originate from the doping effects by the Bi cations.

E. Detailed mechanism of the doping effects

As x increases, the Ru t_{2g} bandwidth should become larger through the hybridization between the Bi $6p$ states and the Ru t_{2g} states.^{8–10,29} However, our optical investigations clearly demonstrated that the hole doping will play a more important role in determining the MIT in the YBRO compounds. How will the Bi substitution result in the hole doping? According to the LDA calculations on the pyrochlore ruthenates by Ishii and Oguchi,⁹ the electron orbitals at the Y site will not be mixed with the Ru t_{2g} orbitals, but the unoccupied Bi $6p$ orbitals should be strongly hybridized with the Ru t_{2g} orbitals. These results imply that the substitution of the Y ion with the Bi ion could give rise to the hole-doping into the Ru t_{2g} bands. In particular, the extended wave function of $6p$ states of the easily polarizable Bi cation makes the self-doping occur.

According to the LDA calculations by Ishii and Oguchi,⁹ an antibonding band of the Tl $6s$ and the O $2p$ orbitals in pyrochlore $\text{Tl}_2\text{Ru}_2\text{O}_7$ is expected to cross E_F , which could provide a self-doping to the Ru t_{2g} states. In our previous optical studies on $\text{Tl}_2\text{Ru}_2\text{O}_7$,^{17,18} we reported an incoherent mid-infrared peak exhibiting unusual temperature dependences. Contrary to the YBRO case, the mid-infrared peak feature could easily be distinguishable from other peaks, and its temperature dependences are similar to the doping dependences of the mid-infrared peak in an externally doped Mott insulator.^{34,35} Therefore, we explained the temperature-dependent MIT of $\text{Tl}_2\text{Ru}_2\text{O}_7$ in terms of a self-doping effect for the Ru ions by the easily polarizable Tl cation.^{17,18} Note that similar self-doping has been observed for Tl- and Bi-based high-temperature superconductors.^{36–39}

It should be also noted that the geometrical frustration of the pyrochlore compounds might play important roles in determining their electronic structures.^{40–42} In the pyrochlore structures where the magnetic ions are located at vertices of

tetrahedra, the antiferromagnetic interaction will experience a strong geometrical frustration. When the frustration is very strong, heavy quasiparticles are formed around the Fermi level by suppressing the short-range antiferromagnetic fluctuations. By decreasing the frustration, the heavy quasiparticle band splits, and the pseudogap begins to develop around the Fermi level. We expect that such geometrical frustration effects could also influence the spectral evolutions of YBRO. Actually, a recent study on the magnetic and electric properties of YBRO by Tachibana *et al.* demonstrated that there exists a strong coupling between charge and spin degrees of freedom, which could be a characteristic feature of a strongly correlated and geometrically frustrated system.⁴³ However, the consideration of such geometrical frustration effects goes beyond our current investigation. Further studies are strongly desirable to understand how the geometrical frustration should modify the electronic structure changes in the bandwidth-control and the filling-control pictures.⁴⁴

VI. SUMMARY

We reported the doping-dependent optical conductivity spectra of the cubic pyrochlore $\text{Y}_{2-x}\text{Bi}_x\text{Ru}_2\text{O}_7$ ($0.0 \leq x \leq 2.0$) and investigated the mechanism of a metal-insulator transition of these alloy compounds. We reported that the spectral features below 5 eV exhibit large changes with a variation of x . We demonstrated that they should be understood in terms of the change in the filling state of the Ru ions. Together with the previous optical studies on $\text{Tl}_2\text{Ru}_2\text{O}_7$,^{17,18} this work suggests that the metallic behaviors of some pyrochlore ruthenates, such as $\text{Bi}_2\text{Ru}_2\text{O}_7$ and $\text{Tl}_2\text{Ru}_2\text{O}_7$ (above 125 K), should be understood in terms of the self-doping for the Ru $4d$ states by the easily polarizable cations, i.e., Bi and Tl.

ACKNOWLEDGMENTS

We would like to thank S. Fujimoto for valuable discussions. This work was supported by the Ministry of Science and Technology through the Creative Research Initiative program, and by KOSEF through the Center for Strongly Correlated Materials Research. The experiments at PLS were supported by MOST and POSCO.

*Present address: Research Center for Materials Science at Extreme Condition, Osaka University, Toyonaka, Osaka 560-8531, Japan.

¹M. A. Subramanian, G. Aravamudan, and G. V. Subba Rao, *Prog. Solid State Chem.* **15**, 55 (1983).

²R. Kanno, Y. Takeda, T. Yamamoto, Y. Kawamoto, and O. Yamamoto, *J. Solid State Chem.* **102**, 106 (1993).

³S. Yoshii and M. Sato, *J. Phys. Soc. Jpn.* **68**, 3034 (1999).

⁴T. Takeda, M. Nagata, H. Kobayashi, R. Kanno, Y. Kawamoto, M. Takano, T. Kamiyama, F. Izumi, and A. W. Sleight, *J. Solid State Chem.* **140**, 182 (1998).

⁵P. A. Cox, R. G. Egdell, J. B. Goodenough, A. Hamnett, and C. C. Naish, *J. Phys. C* **16**, 6221 (1983).

⁶J. B. Goodenough, A. Hamnett, and D. Tjell, in *Localization and M-I Transition*, edited by H. Fritzsche and D. Adler (Plenum, New York, 1985), p. 161.

⁷K.-S. Lee, D.-K. Seo, and M.-H. Whangbo, *J. Solid State Chem.* **131**, 405 (1997).

⁸W. Y. Hsu, R. V. Kasowski, T. Miller, and T.-C. Chiang, *Appl. Phys. Lett.* **52**, 792 (1988).

⁹F. Ishii and T. Oguchi, *J. Phys. Soc. Jpn.* **69**, 526 (2000).

¹⁰J. S. Lee, Y. S. Lee, T. W. Noh, K. Char, Jonghyuk Park, S.-J. Oh, J.-H. Park, C. B. Eom, T. Takeda, and R. Kanno, *Phys. Rev. B* **64**, 245107 (2001).

¹¹J. Okamoto, T. Mizokawa, A. Fujimori, T. Takeda, R. Kanno, F. Ishii, and T. Oguchi, *Phys. Rev. B* **69**, 035115 (2004).

¹²J. Park, K. H. Kim, H.-J. Noh, S.-J. Oh, J.-H. Park, H.-J. Lin, and C.-T. Chen, *Phys. Rev. B* **69**, 165120 (2004).

¹³B. J. Kennedy and T. Vogt, *J. Solid State Chem.* **126**, 261 (1996).

¹⁴B. J. Kennedy, *Physica B* **241–243**, 303 (1998).

- ¹⁵S. L. Cooper, *Struct. Bonding (Berlin)* **98**, 164 (2001), and references therein.
- ¹⁶K. W. Kim, J. S. Lee, T. W. Noh, S. R. Lee, and K. Char, *Phys. Rev. B* **71**, 125104 (2005).
- ¹⁷J. S. Lee, Y. S. Lee, K. W. Kim, T. W. Noh, J. Yu, T. Takeda, and R. Kanno, *Phys. Rev. B* **64**, 165108 (2001).
- ¹⁸J. S. Lee, Y. S. Lee, K. W. Kim, T. W. Noh, J. Yu, Y. Takeda, and R. Kanno, *Physica C* **364–365**, 632 (2001).
- ¹⁹P. Zheng, N. L. Wang, J. L. Luo, R. Jin, and D. Mandrus, *Phys. Rev. B* **69**, 193102 (2004).
- ²⁰T. Yamamoto, R. Kanno, Y. Takeda, O. Yamamoto, Y. Kawamoto, and M. Takano, *J. Solid State Chem.* **109**, 372 (1994).
- ²¹H. Kobayashi, R. Kanno, Y. Kawamoto, T. Kamiyama, F. Izumi, and A. W. Sleight, *J. Solid State Chem.* **114**, 15 (1995).
- ²²S. Yoshii, K. Murata, and M. Sato, *J. Phys. Chem. Solids* **62**, 129 (2001).
- ²³H. J. Lee, J. H. Jung, Y. S. Lee, J. S. Ahn, T. W. Noh, K. H. Kim, and S.-W. Cheong, *Phys. Rev. B* **60**, 5251 (1999).
- ²⁴K. H. Kim, J. Y. Gu, H. S. Choi, D. J. Eom, J. H. Jung, and T. W. Noh, *Phys. Rev. B* **55**, 4023 (1997).
- ²⁵F. Wooten, *Optical Properties of Solids* (Academic Press, New York, 1972).
- ²⁶J. S. Lee, T. W. Noh, J. S. Bae, I.-S. Yang, T. Takeda, and R. Kanno, *Phys. Rev. B* **69**, 214428 (2004).
- ²⁷M. Imada, A. Fujimori, and Y. Tokura, *Rev. Mod. Phys.* **70**, 1039 (1998), and references therein.
- ²⁸Although the t_{2g} bands are not half-filled but 2/3-filled, it could open a Mott gap. In a single-band Hubbard model, the Mott gap should open only at a half-filled state with a critical Coulomb interaction U_c . By the way, if the orbital degeneracy effect is taken into account, it could open at any integer-filled state with U_c , which varies with the number of a band filling. See M. J. Rozenberg, *Phys. Rev. B* **55**, R4855 (1997).
- ²⁹Hyeong-Do Kim, Han-Jin Noh, K. H. Kim, and S.-J. Oh, *Phys. Rev. Lett.* **93**, 126404 (2004).
- ³⁰S. L. Cooper, G. A. Thomas, A. J. Millis, P. E. Sulewski, J. Orenstein, D. H. Rapkine, S.-W. Cheong, and P. L. Trevor, *Phys. Rev. B* **42**, 10785 (1990).
- ³¹Y. Ohta, T. Tohyama, and S. Maekawa, *Phys. Rev. Lett.* **66**, 1228 (1991), and references therein.
- ³²J. S. Lee, Y. S. Lee, T. W. Noh, S. Nakatsuji, H. Fukazawa, R. S. Perry, Y. Maeno, Y. Yoshida, S. I. Ikeda, J. Yu, and C. B. Eom, *Phys. Rev. B* **70**, 085103 (2004).
- ³³In order to address the MIT by analyzing $\sigma(\omega)$, it would also be useful to look into how the coherent spectral weight changes as the MIT occurs. For YBRO, however, it is difficult to estimate the coherent spectral weight since the low energy spectral feature is rather broad and the coherent peak is not well discernable at least up to around $x=1.5$. More detailed studies using the sample with $x>1.5$ would help to address the change of the coherent peak with x .
- ³⁴M. Kasuya, Y. Tokura, T. Arima, H. Eisaki, and S. Uchida, *Phys. Rev. B* **47**, 6197 (1993).
- ³⁵Y. Taguchi, Y. Tokura, T. Arima, and F. Inaba, *Phys. Rev. B* **48**, 511 (1993).
- ³⁶H. Krakauer and W. E. Pickett, *Phys. Rev. Lett.* **60**, 1665 (1988).
- ³⁷L. F. Mattheiss and D. R. Hamann, *Phys. Rev. B* **38**, 5012 (1988).
- ³⁸S. Massidda, J. Yu, and A. J. Freeman, *Physica C* **152**, 251 (1988); J. Yu, S. Massidda, and A. J. Freeman, *ibid.* **152**, 273 (1988).
- ³⁹R. Retoux, F. Studer, C. Michel, B. Raveau, A. Fontaine, and E. Dartyge, *Phys. Rev. B* **41**, 193 (1990).
- ⁴⁰Y. Imai and N. Kawakami, *Phys. Rev. B* **65**, 233103 (2002).
- ⁴¹S. Fujimoto, *Phys. Rev. B* **64**, 085102 (2001); S. Fujimoto, *Phys. Rev. Lett.* **89**, 226402 (2002).
- ⁴²J. Hopkinson and P. Coleman, *Phys. Rev. Lett.* **89**, 267201 (2002).
- ⁴³M. Tachibana, H. Kawaji, and T. Atake, *Phys. Rev. B* **71**, 060402(R) (2005).
- ⁴⁴For $Bi_2Ru_2O_7$, $\sigma(\omega)$ below 1.5 eV is composed of two contributions, i.e., a narrow peak below around 0.1 eV and a broad excitation extending up to around 1.5 eV. (See Fig. 3 of this paper and Fig. 3 of Ref. 18.) Note that the narrow peak below 0.1 eV cannot be attributed to the extrapolation error in the K-K analysis. While the reflectivity was obtained down to 5 meV, different kinds of extrapolation for the reflectivity below 5 meV do not have much effect on the sharp feature around 0.1 eV. Actually, such two-component contribution has been observed in other metallic pyrochlore compounds, such as $Cd_2Re_2O_7$ [N. L. Wang, J. J. McGuire, T. Timusk, R. Jin, J. He, and D. Mandrus, *Phys. Rev. B* **66**, 014534 (2002)] and $Pb_2Ru_2O_{6.5}$ (Ref. 19). A further investigation about this intriguing feature may provide us with an important clue to understanding the electrodynamics of the metallic pyrochlore compounds.